Journal of Molecular Catalysis A: Chemical 300 (2009) 132–141

Contents lists available at ScienceDirect

Journal of Molecular Catalysis A: Chemical

journal homepage: www.elsevier.com/locate/molcata

Palladium-triazine aminoalcohol nanocomposite, its reactivity on Heck reaction

Rocío Redón[a,*], N.G. García-Peña[a], V.M. Ugalde-Saldivar[b], J.J. García[b]

[a] Centro de Ciencias Aplicadas y Desarrollo Tecnológico, Universidad Nacional Autónoma de México, Cd. Universitaria A.P. 70-186, C.P. 04510 Coyoacán, Mexico, D.F., Mexico
[b] Universidad Nacional Autónoma de México, Facultad de Química, Mexico City 04510, D.F., Mexico

ARTICLE INFO

Article history:
Received 27 November 2007
Received in revised form 31 October 2008
Accepted 31 October 2008
Available online 24 November 2008

Keywords:
Palladium nanoparticles
Nanocomposites
Dendrimers
Heck C–C coupling reactions

ABSTRACT

Several studies on dendrimer synthesis and reactivity have been carried out in order to control the size and functionality of compounds. From such studies, it has been suggested that these molecules may be used as ligands to synthesize potential homogeneous catalysts, firstly, in order to get the benefits of both homo- and heterogeneous catalysis (*i.e.* high activity and/or selectivity, good reproducibility, accessibility of the metal site, intermediaries detection, etc.); secondly, because, unlike other polymeric species, they can be readily recoverable after reaction. In this paper, following our interest in homogeneous catalysts, we would like to present our findings from studies on the synthesis and characterization of a prime molecule, triazine aminoalcohol, as starting or zero generation dendrimer and its interaction-reaction with palladium nanoparticles as well as our results on the reactivity on Heck type catalysis.

1. Introduction

Palladium is probably the most versatile metal in promoting or catalyzing reactions, particularly those involving C–C bond formation, many of which are not easily achieved with other transition metal catalysts [1]. It has been found that Pd(0) species systematically and rapidly generated from homogeneous molecular Pd catalysts may eventually aggregate to form Pd nanoparticles (NPs) that can reasonably be suspected to be involved as active species in catalytic processes. Homogeneous and heterogeneous Heck reactions can also be catalyzed by species produced from preformed Pd nanoparticles stabilized by various organic or inorganic stabilizers, in particular tetralkylammonium salts, macromolecules such as dendrimers, ionic liquids, microemulsions, micelles or solid oxides of a variety of elements. The other catalyzed C–C bond formation reactions (Suzuki, Sonogashira, Stille, Corriu–Kumada, Hiyama, Ullman, carbonylation, and Tsuji–Trost allylic substitution) can be catalyzed by Pd nanoparticles, but have been less studied than the Heck reaction except the Suzuki coupling [2]. Another approximation is the use of organometallic compounds as catalysts where metal nanoparticles are suspected to be originated from, like in the Crabtree [3] and other recent tests [4]. Nanoparticle catalysis is one of the most promising solutions toward environmentally friendly catalysis reactions [2]. The properties and catalytic activities of the systems are highly dependent on the supports, methods of preparation, particle size and type and method of preparation of the noble metal. The type of support employed is indeed a critical factor in the performance of the resulting supported material [1]; such supports include oxides such as silicon, aluminum or other metal oxides and forms of carbon supports including carbon nanotubes, or the use of dendrimers that have shown that these macromolecules are the perfect hosts for the catalytically active nanoparticles. The following are examples of some of those studies: Crooks and co-workers' [5] large number of studies on the catalytic behavior of PAMAM dendrimer with palladium nanoparticles, Astruc's [6] research on the case of DAB-dendrimer with Pd(0) NPs, van Leeuwen and co-workers [7] and van Koten and co-workers' [8] synthesis of dendrimers functionalized on the periphery with palladium compounds. Talking about leaching, Rothenberg and Durán [9] wrote: "the nanoparticles suspension is simply a reservoir for metal atoms/ions that leach into solution and that this leaching is now proven for several types of nanoparticle suspensions in various reactions, especially for the catalytically active group palladium metals." In order to solve this problem, there are, at least, three approaches for dealing with it: the first is by immobilizing the nanoparticles on a solid surface; this cuts down the leaching, but also reduces substrate accessibility. Alternatively, by performing biphasic separation using ionic liquids which can minimize leaching while still keeping the nanoparticles accessible. Finally, by using nanoparticle suspensions knowing that leaching occurs and, thereby, maintaining in solution a low concentration of very active homogeneous ligand-free catalysts. The de Vries group has demonstrated this approach for Pd-catalyzed Heck reactions [10].

Thus, following our interest in homogeneous catalysts, in this paper we report the synthesis, characterization and reactivity of a

* Corresponding author. Tel.: +52 55 5622 8602x1154; fax: +52 55 5622 8651.
E-mail address: rredon@servidor.unam.mx (R. Redón).

1381-1169/$ – see front matter © 2008 Elsevier B.V. All rights reserved.
doi:10.1016/j.molcata.2008.10.052

palladium-2,4,6-tris-hydroxyethylamino-1,3,5-triazine nanocomposite on Heck cross-coupling reaction. These catalysts were prepared by mixing Pd(II) with the triazine aminoalcohol zero generation dendrimer in ethylene glycol, which works both as solvent and reducing agent. Palladium NPs prepared in different conditions were used, without the addition of any extra stabilizer, as other authors [11] report.

2. Experimental

2.1. Materials

The manipulation of triazine aminoalcohol zero generation dendrimer was carried out using standard Schlenk and glove box techniques under purified nitrogen. Solvents were degassed and dried using standard procedures. The following were purchased from Sigma–Aldrich and used without further purification: cyanuric chloride (99%), ethanolamine (99.5%), tetrahydrofurane (99+%), N,N-dimethylformamide (DMF) (≥99.9%), ethylene glycol (≥99%), acetonitrile (99%) and $PdCl_2$ (99%). Sodium carbonate (99.6%) was purchased from Baker® ACS, and dried before use. Complex $[PdCl_2(CNCH_3)_2]$ was synthesized by the literature methods [12].

2.2. Instruments

^1H (TMS at 0.0 ppm internal reference) and ^{13}C NMR ($CDCl_3$ at 77 ppm internal reference) experiments were carried out on a Varian *Unity Inova* 400 MHz NMR spectrometer. Elemental analysis was made on a *Fisons EA1108* elemental analyzer. UV–vis absorption spectra, in colloidal dispersion, were determined on an Ocean Optics USB200 miniature fibreglass optic spectrometer. Transmission electron micrographs (TEM) were obtained on a *JEOL 1200EXII* instrument, operating at 60 kV, by deposition of a drop of the colloidal dispersion onto 200-mesh Cu grids coated with carbon/collodion layer. High-resolution transmission electron microscopy (HRTEM) micrographs were obtained on a *JEOL 2000F* instrument, operating at 200 kV, using the same sample preparation as in TEM experiments. The particle size distribution was determined from a digitalized amplified micrograph. Both the catalytic samples and the organic phase were analyzed by gas chromatography (GC/quadrupole, GC–MS). A Varian Saturn3 gas chromatograph with quadrupole detector and db5 capillary column (30 m) was used for quantitative GC analysis. The derivative spectroscopy was carried out on an HP8452A array diode spectrophotometer by means of a 1-cm optical path quartz cuvette. All solutions were made in ethylene glycol as solvent at 1.0 mM concentration. Solutions were measured by using ethylene glycol as blank at 24–48-h intervals after preparation. To perform the quantitative analysis of the species formed, the derivative method was used in order to determine the absorbance values on each of the absorption maximums observed in the region of 300–500 nm. In order to do so, it is necessary to obtain the derivative of the different spectra for further analysis.

2.3. Synthesis

2.3.1. Preparation of triazine aminoalcohol zero generation dendrimer, 2,4,6-tris-hydroxyethylamino-1,3,5-triazine, G0THT

A tetrahydrofurane (50 mL) solution of 1,3,5-trichloro-2,4,6-triazine (2.5 g, 13.55 mmol) with ethanol amine (4.1 mL, 68.13 mmol) and Na_2CO_3 (8.62 g, 81.27 mmol) was heated under reflux for 24 h. The solvent was evaporated and the crude product was filtered and dried under nitrogen, resulting in a purified compound in the form of colorless oil. Yield 2.45 g (70%). ^1H and ^{13}C NMR spectroscopic results are consistent with the formulation proposed. FAB mass spectrometry and elemental analysis results also agree with the proposed formulation. ^1H RMN (400 MHz, $CDCl_3$) δ = 3.58 (t, 2H, CH_2OH), 3.48 (t, 2H, CH_2NHR), 3.36 (s, 1H, OH), 2.64 (t, 1H, NHR). ^{13}C NMR (400 MHz, $CDCl_3$) δ = 168.38 (CN), 60.79 (CH_2OH), 42.34 (CH_2NHR). Anal. Calc. for CHN: C, 48.81; H, 7.02; N, 32.54%. Found C, 48.75; H, 7.06; N, 32.51%.

2.3.2. Preparation of Pd NPs in ethylene glycol

25 mL of $[PdCl_2(CNCH_3)_2]$ 1×10^{-3} M (6.5 mg, 0.025 mmol) solution was prepared in ethylene glycol; in that way, 400 mL solution of 10^{-4} M concentration was obtained after dilution (100 μL from 1×10^{-3} M into 10 mL of ethylene glycol). Then, the solution was stirred while the formation of Pd NPs was monitored by UV–vis absorption spectra.

2.3.3. Preparation of Pd NPs-G0THT in ethylene glycol

A mixture of 1 mL of $[PdCl_2(CNCH_3)_2]$ 1×10^{-3} M (6.5 mg, 0.025 mmol) solution in ethylene glycol (EG) and 24.97 mg (0.1 mmol) of G0THT dendrimer was stirred while the formation of composite was monitored by UV–vis absorption spectra.

2.4. Electrochemical studies

2.4.1. General procedure for the electrochemical measurements

Electrochemical experiments were carried out using a typical three-electrode cell. The vitreous graphite electrode (area: 7.1 mm^2) was used as working electrode, a platinum wire as counter electrode and an $Ag–AgBr/Bu_4NBr_{0.1\ M\ in\ ethylene\ glycol}$ as a pseudo reference. The voltammograms were performed on a PAR263-A potenciostat-galvanostat. All the voltammograms start from an open circuit potential and are obtained in an anodic and cathode sweep. The employed support electrolyte is a Bu_4PF_6 saturated solution in ethylene glycol.

2.5. Catalysis

2.5.1. General procedure for the catalytic reactions

A DMF solution (3 mL) of 5.0 mmol (PhCl: 505 μL, PhBr: 520 μL) of halogen benzene, 6.0 mmol (690 μL) of styrene, and 3.5×10^{-5} mmol of catalyst (1.75 mL of Pd NPs in DMF; 350 μL of Pd NPs in ethylene glycol or 350 μL composite Pd NPs-G0THT dendrimer in ethylene glycol) was introduced into a Schlenk tube in the open air. The tube was charged with a magnetic stir bar and 6 mmol (636 mg) of dry sodium carbonate, sealed, and fully immersed in a 200 °C silicon oil bath. The mixture was refluxed for 20 h. The reaction mixture was filtered through a short plug of celite. The resulting solution was analyzed by gas chromatography (GC/quadrupole, GC–MS). A Varian Saturn3 gas chromatograph with quadrupole detector and db5 capillary column (30 m) was used for quantitative GC analysis.

3. Results and discussion

3.1. Synthesis methods

3.1.1. Preparation of triazine aminoalcohol zero generation dendrimer, 2,4,6-tris-hydroxyethylamino-1,3,5-triazine, G0THT

The synthesis of triazine aminoalcohol zero generation dendrimer G0THT, outlined in Scheme 1, was prepared in a single step from the reaction of 1,3,5-trichloro-2,4,6-triazine with drop wise ethanol amine addition at 0 °C in THF, after addition had finished and temperature had reached room temperature, Na_2CO_3 was added under reflux for 24 h yielded the 2,4,6-tris-hydroxyethylamino-1,3,5-triazine. The purified compound was isolated in 70% yield in the form of colorless oil upon filtration

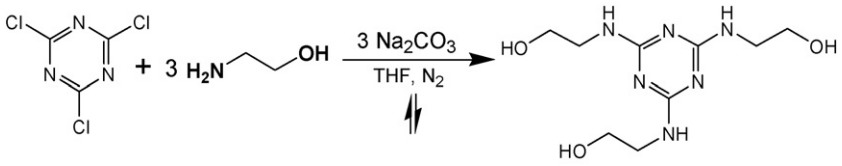

Scheme 1. Synthesis of the G0THT triazine aminoalcohol zero generation dendrimer.

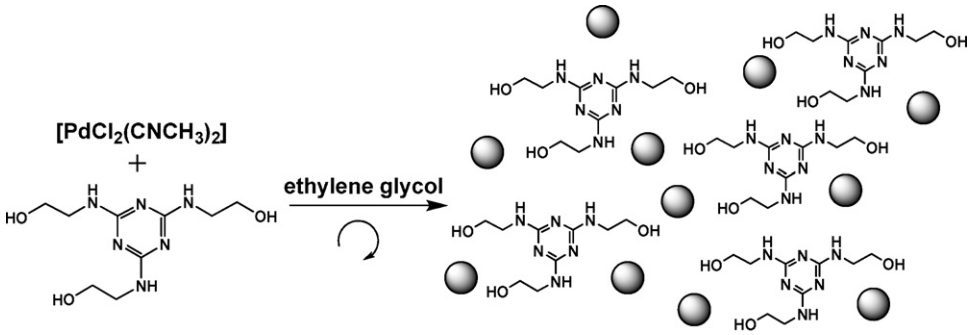

Scheme 2. Preparation of Pd-G0THT nanocomposite.

and solvent elimination under reduced pressure. ^{1}H and ^{13}C NMR spectroscopic results were consistent with the formulation proposed. FAB mass spectrometry and elemental analysis results also agreed with the proposed formulation. The ^{1}H NMR ($CDCl_3$) spectrum showed two sets of triplets at 3.58 ppm (2H) and at 3.48 ppm (2H) which were assigned to the protons on the CH_2OH and CH_2NHR groups, respectively. A broad singlet at 3.36 ppm (1H) assigned to the proton of the O*H* group. A triplet at 2.64 ppm (3H) assigned to the protons of *NH*R triazine group. ^{13}C NMR ($CDCl_3$) exhibited a set of three singlets at 168.38 ppm (1C), at 60.79 ppm (1C) and at 42.34 ppm (1C) assigned to the carbon atoms on the *C*N, CH_2OH and CH_2NHR groups, respectively, as expected for the proposed structure. The FAB mass spectrum showed a peak at 258 *m*/*z* which corresponds to the fragment $[M^+-Cl]$.

3.1.2. Preparation of Pd-G0THT nanocomposite

The nanocomposite was prepared in a different way from the method described by Crooks and co-workers [5], by mixing $[PdCl_2(CNCH_3)]$ with the triazine aminoalcohol in ethylene glycol, without any reducing or stabilizer agent, since the solvent was acting both as reducing and stabilizer (Scheme 2).

3.2. Redox studies

3.2.1. 2,4,6-Tris-hydroxyethylamino-1,3,5-triazine, Pd(II) and ethylene glycol in ethylene glycol

Since the compounds involved in the synthesis of composite Pd-G0THT in ethylene glycol are susceptible to oxide-reduction processes, we carried out a voltammetry study, which will be discussed later in this paper. Fig. 1 shows the graphics corresponding to the voltammetry study of G0THT and Pd(II) in ethylene glycol as solvent. The ethylene glycol graphic shows an oxidation process at 1.8 V/AgBr–Ag (Ia) and its corresponding reduction at −2.00 V (these values are known as "ethylene glycol electro activity domain"). On the other hand, G0THT shows an oxidation process at 1.53 V (I″a) and its corresponding reduction process at 1.12 V (I″c) and a second reduction process at −0.75 V. Since the EG oxidation process appears at 1.8 V (Ia) and the triazine aminoalcohol's at 1.53 V (I″a), it is possible to say that the triazine aminoalcohol is easier to oxidize than the ethylene glycol. From Fig. 1c, it is observed that EG in the presence of Pd(II) proceeds at a lower potential than without the palladium; from 1.8 V without Pd(II) to 1.5 V with Pd(II). In addition, Pd(II) shows two reduction peaks at −0.34 V and −0.73 V (I′c and II′c, respectively). These processes are assigned to two different Pd(II) species coming from the same Pd(0) specie. II′a signal is assigned to palladium adhered to the electrode surface from the I′c reduction process. From the new values of the oxidation potentials at the anode and cathode boundaries (I′a and II′c, respectively), it can be suggested that the presence of Pd(II) favors both the oxidation and reduction EG processes; from 1.8 V to 1.5 V (I′a) in the oxidation process and from −2.0 V to −1.2 V (II′c) for reduction.

The result from the study of the composite Pd-G0THT in EG shows that the reduction/oxidation properties of Pd(II) are modified in presence of the triazine aminoalcohol (Fig. 2). There is an oxidation process observed at 0.25 V/AgBr–Ag (I‴a). The peak at 1.1 V (II‴a) is attributable to the EG oxidation in the presence of Pd(II). There are two reduction signals at 0.22 V and 0.00 V (I‴c and I′c, respectively), one of each is the corresponding reduction

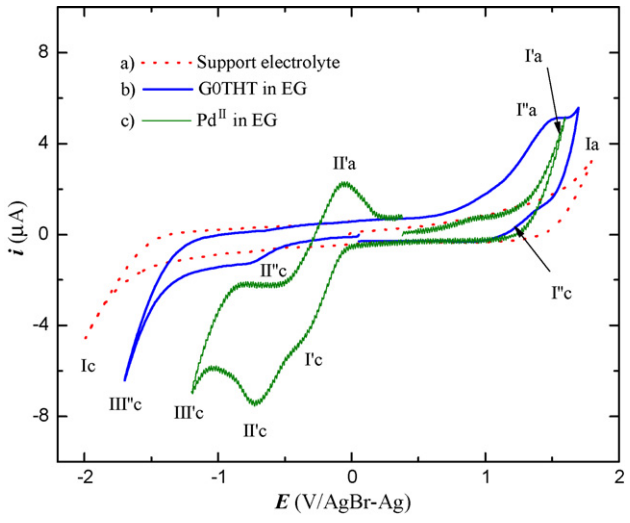

Fig. 1. Typical voltammograms in ethylene glycol at 50 mV s^{-1} on a graphite electrode for (a) saturated solution of Bu_4NPF_6, (b) 0.1 mM G0THT solution in the electrolytic medium, and (c) Pd(II) 1.0 mM solution in the electrolytic medium.

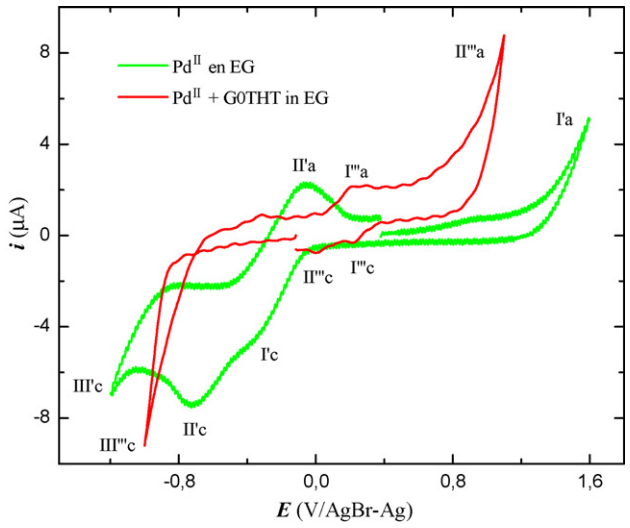

Fig. 2. Typical voltammograms in ethylene glycol at 50 mV s^{-1} on a graphite electrode for Pd(II) 1.0 mM solution in the electrolytic medium and 1:1 mixture of Pd(II) and G0THT solution in the electrolytic medium.

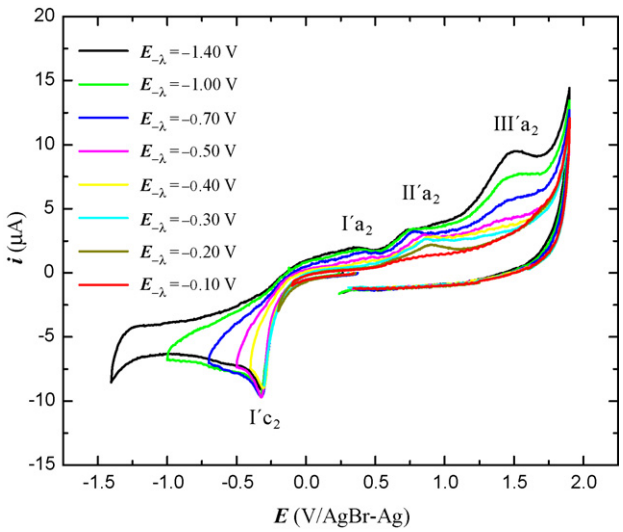

Fig. 3. Typical voltammograms in acetonitrile at 50 mV s^{-1} on a graphite electrode for Pd(II) 1.0 mM solution in the electrolytic medium at different cathodic inversion potentials ($E_{-\lambda}$).

from I‴a oxidation process. It is important to mention that from the very beginning of the voltamperogram $E_{i=0}$ = −0.12 V to 0.83 V, there are no reduction processes assignable to Pd(II), which proves that there are reduction/oxidation modification properties of Pd(II) in the presence of G0THT. These changes are commonly attributed when there is a coordination bonding between both species [13]. Thus, the reduction from Pd(II) to Pd(0) at lower reduction potential value and the easy triazine aminoalcohol oxidation process (I‴a), strongly suggest that there is a new stable coordination compound in solution.

Since, it is not possible to observe the Pd-G0THT reduction process in the study with ethylene glycol as solvent; an additional electrochemical study was made in acetonitrile solvent, which electro activity domain is wider.

3.2.2. 2,4,6-Tris-hydroxyethylamino-1,3,5-triazine, Pd(II) and ethylene glycol in acetonitrile

The characterization of each species in acetonitrile gives the following results: the triazine aminoalcohol voltammogram in acetonitrile (Figure S1, supplementary material) shows a single irreversible oxidation signal from anodic potential at E_{pa} = 1.76 (V/AgBr–Ag); EG also shows a single oxidation signal at E_{pa} = 1.78 (V/AgBr–Ag) and a reduction signal at cathode potential of E_{pc} = −1.54 (V/AgBr–Ag). In Fig. 3, the typical voltammograms from a 1 mM solution of Pd(II) in a Bu_4NPF_6 0.1 M solution in acetonitrile can be observed. The graphics correspond to a study of variable cathode inversion potential ($E_{-\lambda}$) where it is possible to observe a characteristic reduction signal from Pd(II) to Pd(0) (I′c$_2$, E_{pc} = 0.33 V). There are other three oxidation peaks (I′a$_2$, II′c$_2$, and III′a$_2$) which depend on the inversion potential and are assigned to three different Pd(II) species that are formed during the Pd(0) oxidation deposited in the electrode. These signals do not appear when the potential run starts in the anodic way. Thus, they are associated to oxidation processes in the electrode, which will be discussed elsewhere.

The reduction from Pd(II) to Pd(0) in absence of EG signal appears at a very similar potential (E_{pc} = −0.27 V and E_{pc_2} = −0.33 V for Pd(II)-EG and Pd(II), respectively) (Fig. 4). This suggests that EG has a small effect on the redox properties of Pd(II). As it can be seen in the voltammograms shown in Fig. 4, there are modifications in the oxidation signals; nevertheless, they will not be discussed here, since they are oxidation processes occurred in the palladium electrode.

A comparison of the electrochemical behavior of an 1:1 composite Pd(II):G0THT with that of Pd(II) alone in acetonitrile (Fig. 5) revealed that the corresponding reduction to Pd(II)-G0THT is at E_{pc_3} = −0.73 V, shifted 0.4 V from Pd(II) alone in acetonitrile. In conclusion, the so-far obtained results allows to say that (i) both the ethylene glycol and the triazine aminoalcohol are oxidation susceptible with Pd(II); (ii) Pd(II) is reduced to Pd(0) in the process; (iii) the results from the composite Pd-G0THT electrochemical behavior agree with the observation of the synthesis of nanocomposite Pd NPs-G0THT in ethylene glycol, since the nanoparticles synthesis is faster in EG than in the presence of G0THT which is attributable to the fact that a slower redox process occurs between Pd(II) and G0THT than between Pd(II) and the ethylene glycol. There are several examples which show that the oxidation power of a redox system diminishes when there are coordination compounds

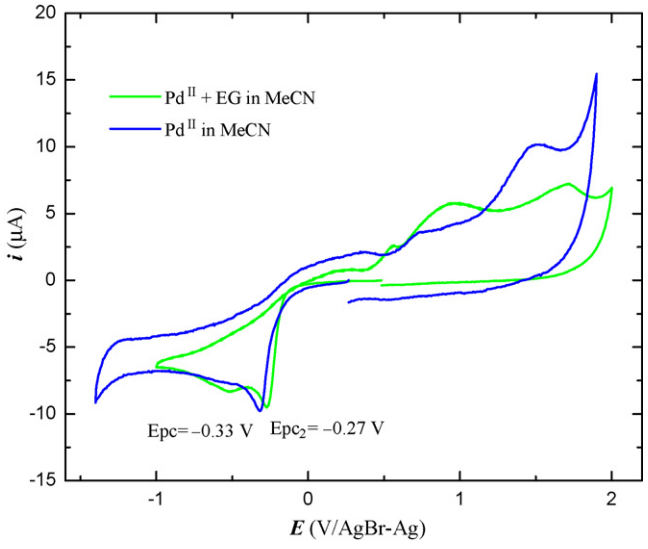

Fig. 4. Typical voltammograms in acetonitrile at 50 mV s^{-1} on a graphite electrode for Pd(II) 1.0 mM solution in the electrolytic medium and 1:1 mixture of Pd(II) and ethylene glycol solution in the electrolytic medium.

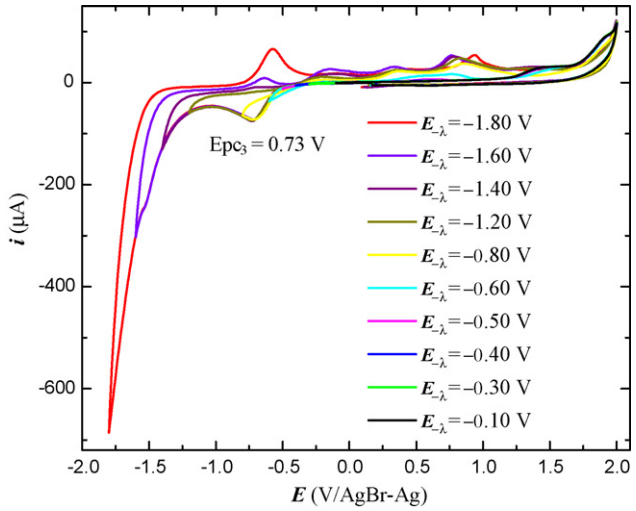

Fig. 5. Typical voltammograms in acetonitrile at 50 mV s^{-1} on a graphite electrode for Pd(II) 1.0 mM solution in the electrolytic medium and 1:1 mixture of Pd(II) and G0THT solution in the electrolytic medium.

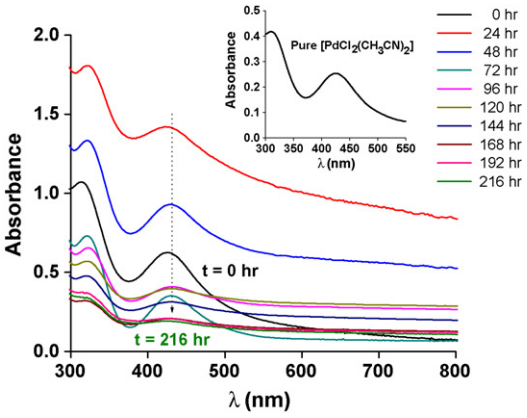

Fig. 6. UV–vis spectra during the reduction of Pd(II) with ethylene glycol. The inset shows the spectrum of pure $[PdCl_2(CH_3CN)_2]$ in ethylene glycol.

formation equilibriums with the oxidant [13], in this case with Pd(0).

3.3. UV–vis electronic absorption spectroscopy

The palladium clusters were synthesized in solution using the solvent both as reducing agent and as a stabilizer. In a typical reaction (Eq. 1) the Pd salt precursor was dissolved and let react through time. Reaction progress was monitored by UV–vis spectrometry (Fig. 6). We observed some bulk metal precipitation at the end of the reaction which gave the optical precipitation that can be observed on the 4-h spectrum. Fig. 6 shows the time-resolved spectra for Pd cluster formation. Pure $[PdCl_2(CH_3CN)_2]$ in ethylene glycol showed two maxima at 314 nm and 426 nm, respectively. As the reaction proceeded, Pd(II) ions were reduced to Pd(0) atoms and further grew to form clusters. This transition decreased the absorbance at 426 nm, and the band at 314 nm shifted to 321 nm.

Some metal nanoparticles such as Ag and Au absorb photons in the UV–vis region due to a coherent oscillation of the conduction band electrons induced by the interacting electromagnetic fields. These resonances are known as surface plasmons [14]. Several transition metals, including Pd, do not show pronounced surface plasmon peaks due to *d–d* interband transitions. In our case, we observed that the absorption at 321 nm corresponds to the formation of Pd nanoclusters [15]. Using transmission electron microscopy (TEM), we found that the above synthesis procedure gives 20.7 ± 8.3 nm and 3.8 ± 2.7 nm clusters (Fig. 7). In spite of, the observation of such variations in the absorption intensity of both signals, a precise estimation of those changes cannot be made due to the baseline shifts caused by the formation of solid particles suspended in the colloid suspension. Thus, it was necessary to determine each spectrum derivative at different times (Figure S3, supplementary material) and calculate the difference between regions I-II and III-IV on the derivative spectrum in Figure S3. The delta (Δ) found in region I-II corresponds to the amount of Pd(0) nanoparticles and the Δ found in region III-IV corresponds to the amount of Pd(II) in solution. When such Δ values are expressed in terms of time (Figure S4), the following can be conclude: (a) the Pd(0) nanoparticle dispersed in EG solution reaches a maximum after 4 days then, a decay is observed because the clusters are big enough to precipitate throughout time; additionally, its quantity also increases as days go by and the amount of Pd NPs in solution decreases and (b) Pd(II) in solution is reduced to Pd(0) with ethylene glycol, thus, disappearance of Pd(II) in solution occurs from the beginning to near the end of the observation period. This was confirmed through a time-based electrochemical study of the same solution (Figure S5, supplementary material), which proves that the amount of Pd(II) almost completely decreases on observation day 9 (*vide infra*).

In the same manner in which palladium nanoclusters were synthesized, we prepared nanocomposites by two approximations; first, we prepared the G0THT and palladium solutions separately,

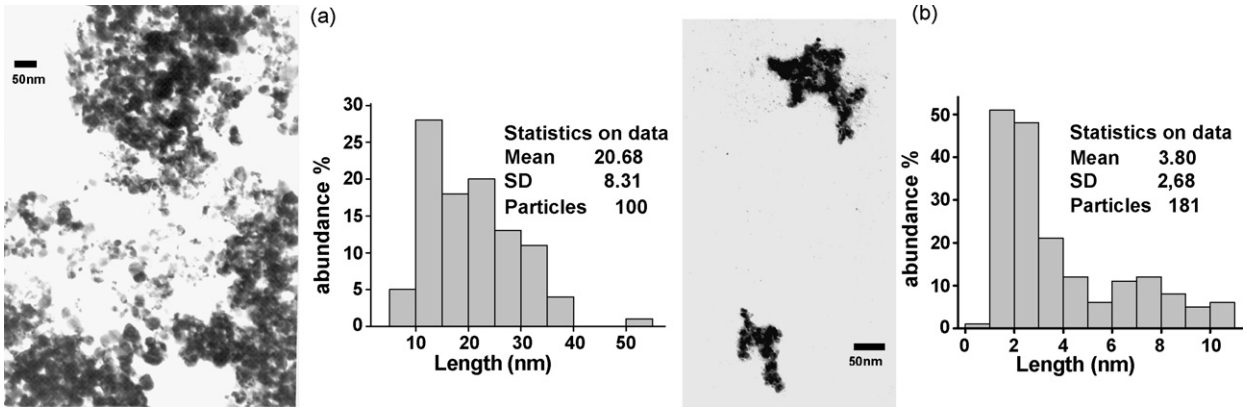

Fig. 7. Transmission electron micrographs and corresponding size distribution of Pd clusters prepared by reducing $[PdCl_2(CNCH_3)_2]$ with ethylene glycol: (a) large particles distribution and (b) isolated clusters in ethylene glycol.

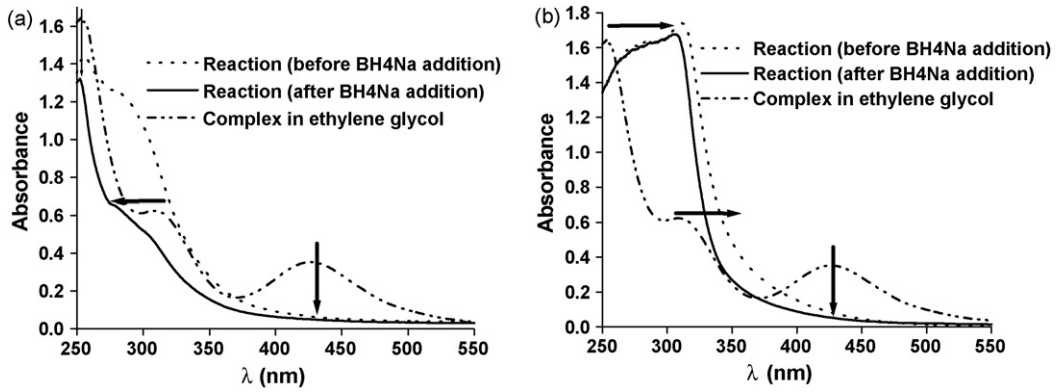

Fig. 8. UV–vis spectra of the reduction of Pd(II) with $NaBH_4$ in ethylene glycol: (a) from the solutions of Pd NPs and G0THT prepared separately before $NaBH_4$ addition and (b) from a solution of the nanocomposite Pd NPs-G0THT in the same flask before borohydride addition.

then we mixed them and, finally, we added a solution of $NaBH_4$ at the end of the synthesis, obtaining the graphic in Fig. 8a. As the reaction proceeded, Pd(II) ions were partially reduced to Pd(0) atoms, the band showing strong absorption up to ~314 nm shifted to ~306 nm and the one at 253 nm shifted to 270 nm, suggesting the formation of palladium clusters (colloidal palladium) [15], and the band of 426 nm assigned to Pd(II), disappeared. In this case, we did not observe any bulk metal precipitation, which might be attributable to the complexation of Pd(II) and/or Pd(0) particles with OH and/or NH groups from the triazine aminoalcohol, which matches with the results obtained on redox analysis, *vide supra*. Using HRTEM, we found that the above procedure gave Pd(II) and Pd(0) nanoparticle clusters with diameters of 2.18 ± 0.33 nm and 4.08 ± 0.66 nm (Fig. 9a and b). On the second approximation, we prepared a solution of G0THT and the palladium complex in the same flask and then we added the solution of $NaBH_4$ at the end of the synthesis, obtaining the graphic in Fig. 8b. In this case, the graphics were quite similar after and before the $NaBH_4$ addition, with a small shift from the 253 nm band to 312 nm before the borohydride addition, and to 306 nm after the addition, as well as the consequent disappearance of the 426 nm absorption assigned to Pd(II). This suggests that there is a reduction from Pd(II) to Pd(0) by the triazine aminoalcohol in ethylene glycol without the necessity of the borohydride.

3.4. Microscopy studies

From the different zones analyzed in TEM experiments, we can suggest that the triazine aminoalcohol molecules are localized in a preferential orientation which generates large structures that contain Pd nanoparticles distributed along them (Fig. 10). This conclusion is based not only on TEM analysis but also on high-resolution images which will be explained in detail. Fig. 11a shows the typical contrast of the graphite layers where the average interplanar

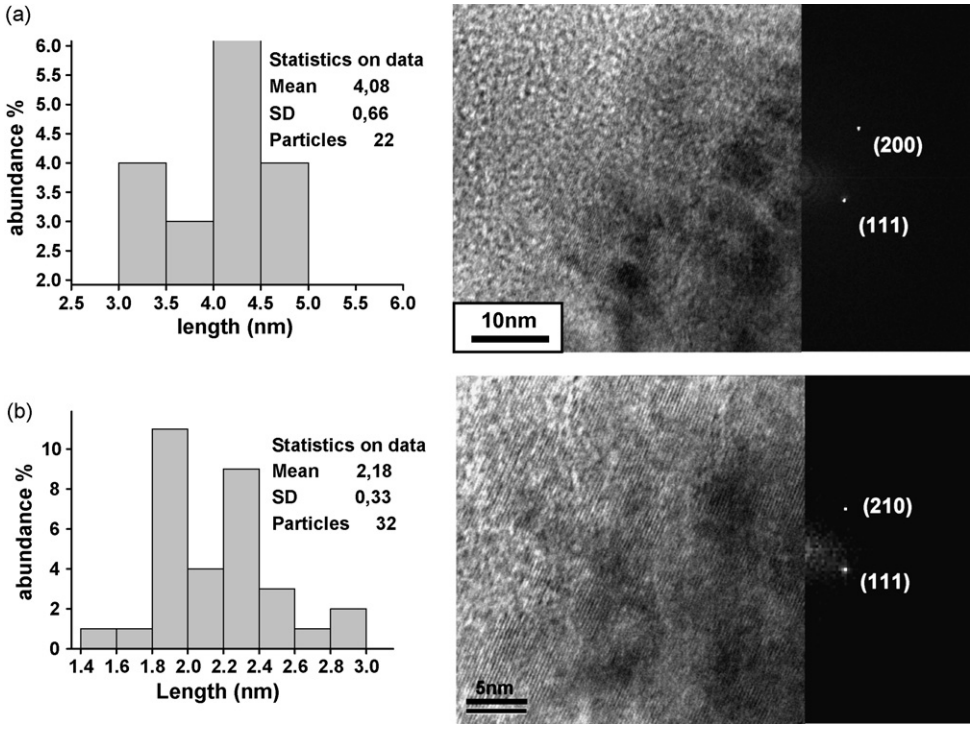

Fig. 9. HRTEM images of nanocomposite Pd-G0THT: (a) Pd(0) nanoparticles and (b) Pd(II) nanoparticles.

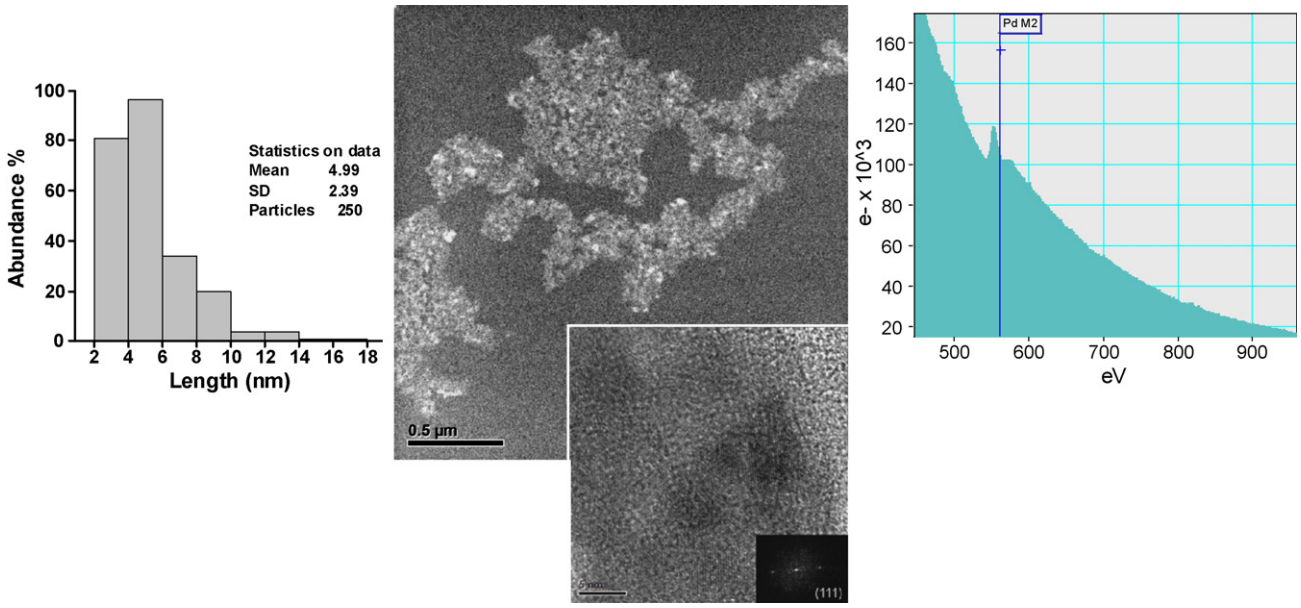

Fig. 10. Z-contrast TEM image micrograph with HRTEM from the palladium nanoparticles inside G0THT (middle): corresponding size distribution of Pd clusters–lighter zones (left) and the corresponding EELS that shows palladium inside the triazine aminoalcohol.

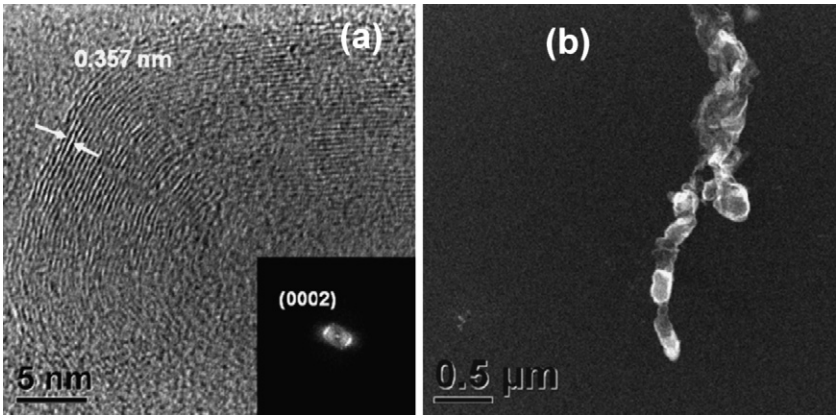

Fig. 11. (a) Typical contrast of the graphite layers. The average interplanar distance corresponds to 0.357 nm, this can be the carbon layers associated to the triazine aminoalcohol structures; (b) a hollow carbon structure found in a lacey carbon grid. The depth focus characteristic for the Z-contrast images allows observing the hollow structure.

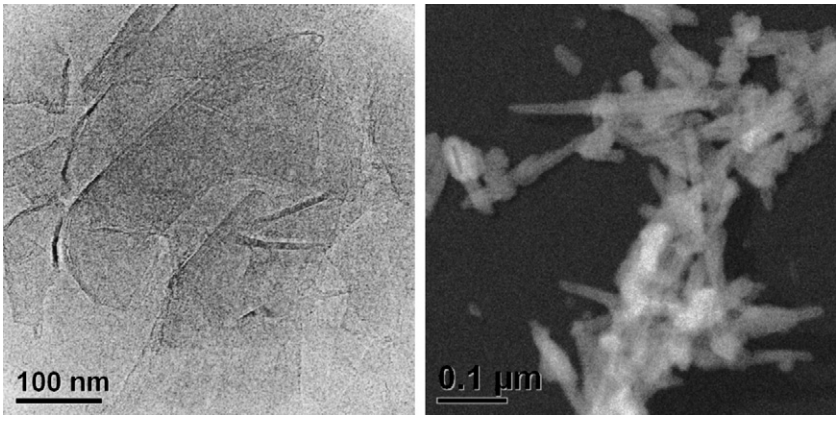

Fig. 12. Conventional TEM micrograph (left) and the corresponding Z-contrast image from a zone with polyhydric graphite structures.

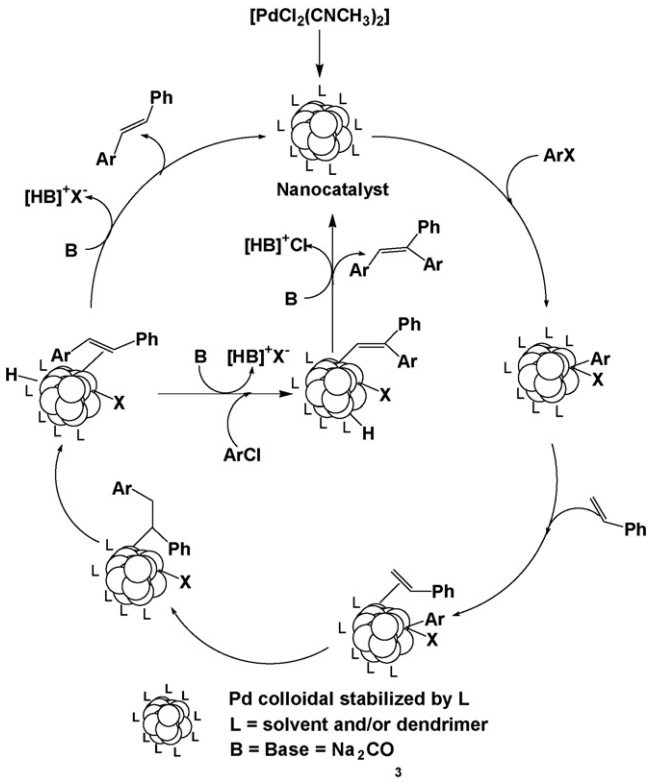

Scheme 3. Proposed catalytic mechanism.

distance corresponds to 0.357 nm which is more relaxed than the one corresponding to 0.339 nm for the interplanar distance for the 2H hexagonal graphite. These can be the carbon layers associated to the G0THT structures. Fig. 11b corresponds to a hollow carbon structure found in a lacey carbon grid. The depth focus characteristic of the Z-contrast images allows to observe the hollow structure; additionally, the polyhydric graphite structures shown in Fig. 12 also support the idea of the presence of G0THT structures [16]. On the other hand, in Z-contrast analysis (Fig. 10), there is also evidence of Pd (lighter zones) immersed in the triazine aminoalcohol structures. As the particles are immersed in the triazine aminoalcohol structure, it is difficult to observe them clearly; nevertheless, it was possible to obtain some measurements determining an average size of 4.99 ± 2.39 nm, which are consistent with high-resolution images of Pd(II) and Pd(0) nanoparticles with diameters of 2.18 ± 0.33 nm and 4.08 ± 0.66 nm (Fig. 9). A comparison between nanoparticle diameters without stabilizing agents but the solvent (20.7 ± 8.3 nm and 3.8 ± 2.7 nm, Fig. 10) and those from the composite showed that the dendrimer was working as stabilizer.

3.5. Catalytic studies

3.5.1. Catalytic activity of Pd-G0THT composite for the Heck coupling of aryl halides with olefins

The effect of G0THT in the catalytic activity is analyzed by comparing the synthesized nanocomposite with the different systems of Pd NPs obtained.

The catalytic performance of the Pd-G0THT composite was examined in the Heck reaction between chloro or bromobenzene and styrene (Scheme 3). The results are gathered in Table 1. From the results with NPs obtained in ethylene glycol, it can be seen that the increment in the reaction time results in a higher specificity of the reaction: decreasing the amount of the trisubstituted (*T*)

Table 1
Heck couplings of halobenzenes with different nanospecies as catalysts.

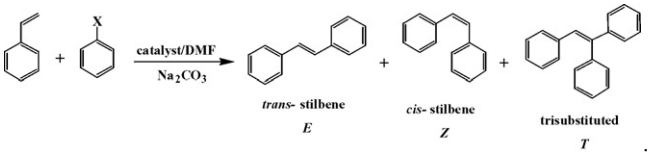

Catalyst[a]	X	Yield (%)[b]	*E* (%)	*Z* (%)	*T* (%)
G0THT[b]	Cl	–	–	–	–
G0THT	Br	–	–	–	–
Pd NP 0.5 h	Cl	66.35	57.79	–	8.56
Pd NP 0.5 h	Br	>99.90	66.48	33.52	–
Pd NP 1 h	Cl	70.20	62.84	–	7.36
Pd NP 1 h	Br	96.23	79.33	16.90	–
Pd NP 2 h	Cl	62.93	62.93	–	–
Pd NP 2 h	Br	99.84	98.96	0.88	–
Pd NP 3 h	Cl	95.95	80.76	–	15.19
Pd NP 3 h	Br	99.48	98.56	0.92	–
Pd NP/$NaBH_4$, 3 h	Cl	93.49	36.96	–	56.53
Pd NP/$NaBH_4$, 3 h	Br	96.98	16.13	–	80.85
Pd NP-G0THT	Cl	80.39	72.49	–	7.90
Pd NP-G0THT	Br	97.37	81.24	16.13	–
NP-G0THT-BH_4[c] *in situ*	Cl	98.38	32.67	–	65.71
NP-G0THT-BH_4[c] *in situ*	Br	>99.90	95.03	2.34	2.63
NP-G0THT-BH_4[d]	Cl	96.67	35.19	–	61.48
NP-G0THT-BH_4[d]	Br	98.72	93.43	2.87	2.42

Reaction conditions: 5 mmol of halobenzene, 6 mmol of styrene, 6 mmol of base, 3.5×10^{-5} mmol of catalyst and 3 mL of DMF, 20 h at 200 °C.

[a] All the catalysts are prepared in ethylene glycol solution.

[b] Yields obtained by GC are based on haloarene and are the average of two runs. Conversions and yields were calculated on the GC area by incorporating an internal standard.

[c] From a solution of the nanocomposite Pd NPs-dendrimer in the same flask before borohydride addition.

[d] From the solutions of Pd NPs and dendrimer prepared separately before $NaBH_4$ addition.

product and increasing the production of *trans*-stilbene (*E*) when Pd NPs obtaining time reaches 2 h, where there is no *T* product at all. On the other hand, in the reaction with bromobenzene, the production of *cis*-stilbene (*Z*) also decreases with the consequent increment of *E*. When Pd NPs obtaining time reaches 3 h, these percentages increase, which means that the size of the NPs is no longer appropriate for the specificity of the reaction (Fig. 13). This result strongly suggests that the nanoparticles size and environment are key factors for the catalysis reactions.

In comparison with these results, when nanocomposite Pd-G0THT is used as a catalyst without the addition of borohydride, there is a medium percentage production of *T* and *Z* products for chloro and bromobenzene reactions, respectively. This takes us to the conclusion that the size of the nanoparticles reached inside the dendrimer is in between those obtained for the NPs alone; nevertheless, as they are inside the dendrimer, this size will remain constant and the products obtained will be the same, no matter how long the composite remains in solution.

When $NaBH_4$ is added to the composite, the complete reduction of all Pd(II) is assured, thus, there is a better selectivity, indicating that only Pd(0) is participating in the catalyst reaction and that the presence of Pd(II) from the very beginning in the reaction diminishes its selectivity and yield. Nevertheless, both the yield and selectivity are better on the 2 h NPs-EG as catalyst reaction; the size increment of the NPs is avoided with the presence of the dendrimer.

A number of articles describing the use of palladium nanoparticles or composites with them as catalysts have been published; most of them employed bromo and iodoarenes in C–C coupling reactions with yields from 76% to 100% [17–32]. Rarely, these catalysts were able to activate chloroarenes [33] and, in such cases,

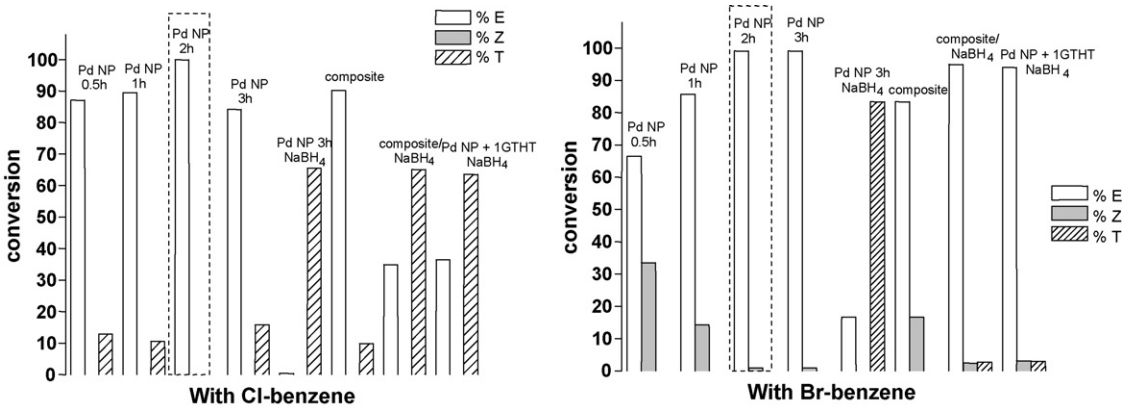

Fig. 13. Graphics of catalytic results: (left) with chlorobenzene as halobenzene; (right) with bromobenzene. In both cases it is easy to see that the presence of Pd(II) favors the production of additional isomers, *T* for chlorobenzene and *Z* for bromobenzene. Pd NPs obtained at 2 h in ethylene glycol, show the best yield and selectivity in both cases.

there were informed yields of 1%, 51% [34] and 94% using NBu_4Br as additive [33]. In our case, we are achieving 98% yield without any additive. In addition, the catalytic composite is stable in solution for long periods of time.

The precise mechanism of the catalytic reaction needs to be elucidated, but it is noticeable that the mechanism is strongly modified depending of the halobenzene employed, obtaining in both cases *trans*-stilbene as the main product, trisubstituted product for chlorobenzene reaction and *cis*-stilbene for bromobenzene reaction, either with the nanocomposite or with NPs as catalysts. There is still a debate in the literature about the oxidation states of the species involved in the cycle (Scheme 3) with Pd(IV)/Pd(II) and Pd(II)/Pd(0), both being suggested several times [35]. Nonetheless, as it is the case in other examples of Heck catalyst employing nanoparticles [36], we favor the Pd(0)/Pd(II) mechanism since the species that we detect are in these oxidation states, either with redox studies or by electronic diffraction form HRTEM analysis (Figs. 4, 9a and b, and 10), although participation of Pd(IV)/Pd(II) species cannot be ruled out.

4. Summary

In conclusion, we have prepared a composite nanoparticle generation-0 dendrimer for catalyst applications in which the dendrimer is employed both as template and stabilizer. Both the ethylene glycol and the dendrimer are oxidation susceptible with Pd(II). During the process, Pd(II) is reduced to Pd(0). The results from the composite Pd-G0THT electrochemical behavior agree with the observation of the synthesis of the nanocomposite Pd NPs-G0THT in ethylene glycol. Since a slower redox process occurs between Pd(II) and the dendrimer than between Pd(II) and ethylene glycol, the nanoparticles synthesis is faster in EG than with the dendrimer and, thus the nanoparticles are smaller in the presence of the dendrimer.

The composite as a catalyst is a very good stabilizer of the nanoparticles size and gets a good *E* selectivity mainly with bromobenzene in Heck type C–C coupling reaction, principally attributed to the nanoparticle size reached inside the dendrimer. As the nanoparticles are inside the dendrimer, this size will remain constant and the products obtained will be the same, no matter how long the composite remains in solution, since the particles are quite stable, but accessible enough to substrates in solution. Finally, the composite is able to activate the chlorobenzene in the conditions used for the Heck reaction. The influence of the dendrimer generation is still under research.

Acknowledgments

Financial support for this research by CONACyT (J43116-F) and PAPIIT (IN106405 and IN101308) is gratefully acknowledged. Helpful suggestions from the reviewers are also greatly appreciated.

Appendix A. Supplementary data

Supplementary data associated with this article can be found, in the online version, at doi:10.1016/j.molcata.2008.10.052.

References

[1] A. Barau, V. Budarin, A. Caragheorgheopol, R. Luque, D.J. Macquarrie, A. Prelle, V.S. Teodorescu, M. Zaharescu, Catal. Lett. 124 (2008) 204, and references therein.
[2] D. Astruc, Inorg. Chem. 46 (2007) 1884, and references therein.
[3] D.R. Anton, R.H. Crabtree, Organometallics 2 (1983) 855.
[4] (a) J.A. Widegren, R.G. Finke, J. Mol. Catal. A: Chem. 198 (2003) 317;
(b) I.W. Davies, L. Matty, D.L. Hughes, P.J. Reider, J. Am. Chem. Soc. 123 (2001) 10139.
[5] (a) O.M. Wilson, M.R. Knecht, J.C. Garcia-Martinez, R.M. Crooks, J. Am. Chem. Soc. 128 (2006) 4510;
(b) S.K. Oh, Y.H. Niu, R.M. Crooks, Langmuir 21 (2005) 10209;
(c) J.C. Garcia-Martinez, R. Lezutekong, R.M. Crooks, J. Am. Chem. Soc. 127 (2005) 5097;
(d) R.W.J. Scott, H.C. Ye, R.R. Henriquez, R.M. Crooks, Chem. Mater. 15 (2003) 3873;
(e) R.W.J. Scott, O.M. Wilson, R.M. Crooks, J. Phys. Chem. B 109 (2005) 692;
(f) Y.H. Niu, R.M. Crooks, C. R. Chim. 6 (2003) 1049;
(g) M.Q. Zhao, R.M. Crooks, Angew. Chem. Int. Ed. 38 (3) (1999) 364.
[6] J. Lemo, K. Heuze, D. Astruc, Inorg. Chim. Acta 359 (2006) 4909.
[7] (a) J.N.H. Reek, S. Arevalo, R. van Heerbeek, P.C.J. Kamer, P.W.N.H. van Leeuwen, Adv. Catal. 49 (2006) 71;
(b) D. de Groot, J.N.H. Reek, P.C.J. Kamer, P.W.N.M. van Leeuwen, Eur. J. Org. Chem. (2002) 1085.
[8] (a) R. van de Coevering, P.C.A. Bruijnincx, C.A. van Walree, R.J.M.K.G. van Koten, Eur. J. Org. Chem. (2007) 2931;
(b) R. van de Coevering, P.C.A. Bruijnincx, M. Lutz, A.L. Spek, G. van Koten, R.J.M.K. Gebbink, New J. Chem. 31 (2007) 1337;
(c) R. van de Coevering, A.P. Alfers, J.D. Meeldijk, E. Martinez-Viviente, P.S. Pregosin, R.J.M. Gebbink, G. van Koten, J. Am. Chem. Soc. 128 (2006) 12700.
[9] L. Durán Pachón, G. Rothenberg, Appl. Organomet. Chem. 22 (2008) 288.
[10] A.H.M. de Vries, F.J. Parlevliet, L. Schmieder-van de Vondervoort, J.H.M. Mommers, H.J.W. Henderickx, M.A.M. Walet, J.G. de Vries, Adv. Synth. Catal. 344 (2002) 996.
[11] (a) R. Narayanan, M.A. El-Sayed, Chim. Oggi. 25 (2007) 84;
(b) R. Narayanan, M.A. El-Sayed, J. Catal. 234 (2005) 348;
(c) R. Narayanan, M.A. El-Sayed, J. Phys. Chem. B 109 (2005) 12663;
(d) R. Narayanan, M.A. El-Sayed, Langmuir 21 (2005) 2027;
(e) R. Narayanan, M.A. El-Sayed, Nano Lett. 4 (2004) 1343;
(f) R. Narayanan, M.A. El-Sayed, J. Phys. Chem. B 108 (2004) 8572;
(g) R. Narayanan, M.A. El-Sayed, J. Am. Chem. Soc. 126 (2004) 7194;
(h) R. Narayanan, M.A. El-Sayed, J. Phys. Chem. B 108 (2004) 5726;
(i) R. Narayanan, M.A. El-Sayed, J. Am. Chem. Soc. 125 (2003) 8340;

(j) Y. Li, E. Boone, M.A. El-Sayed, Langmuir 18 (2002) 4921;
(k) Y. Li, M.A. El-Sayed, J. Phys. Chem. B 105 (2001) 8938;
(l) Y. Li, X.M. Hong, D.M. Collard, M.A. El-Sayed, Org. Lett. 2 (2000) 2385;
(m) J.M. Petroski, Z.L. Wang, T.C. Green, M.A. El-Sayed, J. Phys. Chem. B 102 (1998) 3316;
(n) D. Astruc, Inorg. Chem. 46 (2007) 1884;
(o) D. Mery, D. Astruc, Coord. Chem. Rev. 250 (2006) 1965;
(p) D. Astruc, F. Lu, J.R. Aranzaes, Angew. Chem. Int. Ed. 44 (2005) 7852;
(q) D. Astruc, C. R. Chim. 8 (2005) 1101;
(r) J. Lemo, K. Heuze, D. Astruc, Org. Lett. 7 (2005) 2253;
(s) D. Astruc, K. Heuze, S. Gatard, D. Mery, S. Nlate, L. Plault, Adv. Synth. Catal. 347 (2005) 329;
(t) Z.H. Zhang, Z.G. Zha, C.S. Gan, C.F. Pan, Y.Q. Zhou, Z.Y. Wang, M.M. Zhou, J. Org. Chem. 71 (2006) 4339.
[12] G.K. Anderson, M. Lin, Inorg. Synth. 28 (1990) 60.
[13] V.M. Ugalde-Saldivar, M.E. Sosa-Torres, I. Gonzalez, Eur. J. Inorg. Chem. 5 (2003) 978–987.
[14] N.A. Kotov (Ed.), Nanoparticle Assemblies and Superstructures, vol. 8, U.S. Taylor & Francis Group, 2006.
[15] A. Creighton, D.G. Eadon, Chem. Soc. Faraday Trans. 87 (1991) 3881.
[16] D. Mendoza, P. Santiago, Rev. Mex. de Fis. S 53 (2007) 9.
[17] X. Yang, Z.F. Fei, T.J. Geldbach, A.D. Phillips, C.G. Hartinger, Y.D. Li, P.J. Dyson, Organometallics 27 (2008) 3971.
[18] A. Barau, V. Budarin, A. Caragheorgheopol, R. Luque, D.J. Macquarrie, A. Prelle, V.S. Teodorescu, M. Zaharescu, Catal. Lett. 124 (2008) 204.
[19] J.Z. Jiang, C. Cai, J. Colloid Interf. Sci. 307 (2007) 300.
[20] N. Panziera, P. Pertici, L. Barazzone, A.M. Caporusso, G. Vitulli, P. Salvadori, S. Borsacchi, M. Geppi, C.A. Veracini, G. Martra, L. Bertinetti, J. Catal. 246 (2007) 351.
[21] N. Ren, Y.H. Yang, Y.H. Zhang, Q.R. Wang, Y. Tang, J. Catal. 246 (2007) 215.
[22] H. Tanaka, S. Koizumi, T. Hashimoto, H. Itoh, M. Satoh, K. Naka, Y. Chujo, Macromolecules 40 (2007) 4327.
[23] S. Tandukar, A. Sen, J. Mol. Catal. A: Chem. 268 (2007) 112.
[24] W.B. Yi, C. Cai, X. Wang, J. Mol. Catal. A: Chem. 274 (2007) 68.
[25] I.P. Beletskaya, Q.R. Khokhlov, E.A. Tarasenko, V.S. Tyurin, J. Organomet. Chem. 692 (2007) 4402.
[26] G. Budroni, A. Corma, H. Garia, A. Primo, J. Catal. 251 (2007) 345.
[27] A.K. Diallo, C. Ornelas, L. Salmon, J.R. Aranzaes, D. Astruc, Angew. Chem. Int. Ed. 46 (2007) 8644.
[28] I.P. Beletskaya, A.N. Kashin, A.E. Litvinov, V.S. Tyurin, P.M. Valetsky, G. van Koten, Organometallics 25 (2006) 154.
[29] A. Corma, H. Garcia, A. Leyva, J. Catal. 240 (2006) 87.
[30] H. Hagio, M. Sugiura, S. Kobayashi, Org. Lett. 8 (2006) 375.
[31] B. Karimi, D. Enders, Org. Lett. 8 (2006) 1237.
[32] C.C. Luo, Y.H. Zhang, Y.G. Wang, J. Mol. Catal. A: Chem. 229 (2005) 7.
[33] K. Klaus, K. Wolfgang, S. Sandra Pröckl, Inorg. Chem. 46 (2007) 1876.
[34] P.W. Zheng, W.Q. Zhang, J. Catal. 250 (2007) 324.
[35] (a) C. Luo, Y. Zhang, Y. Wang, J. Mol. Catal. A: Chem. 229 (2005) 7;
(b) J. Hu, Y.B. Liu, Langmuir 21 (2005) 2121.
[36] (a) D. Morales-Morales, R. Redon, Y.F. Zheng, J.R. Dilworth, Inorg. Chim. Acta 328 (2002) 39;
(b) A.M. Trzeciak, J.J. Ziolkowski, Coord. Chem. Rev. 251 (2007) 1281.